Journal of Computational Methods in Sciences and Engineering 6 (2006) S389–S398
IOS Press

Response of magnetostrictive smart structures to sinusoidal and step force inputs

Sultan Aljahdali[a,*] and Syed J. Hyder[b]
[a]*School of Information Technology, George Mason University, Fairfax, VA, 22030, USA*
[b]*Department of Health Information Management, Batterjee Medical College, P.O. Box 2550, Jeddah 21461, Saudi Arabia*

Abstract. Constitutive equations of magnetostrictive smart materials involving mechanical and magnetic fields are presented via Hamilton's principle. Finite element equations are used to solve the equations of motion subjected to different force inputs. Magnetostrictive ($CoFe_2O_4$) layers mounted on the root of cantilever beam is considered as the case study to obtain the displacement and magnetic response both in the X and Y directions when subjected to sinusoidal and step force inputs. Fast Fourier Transformation (FFT) technique is also employed to obtain the Power Spectral Density (PSD) of displacement and magnetic responses in both X and Y directions.

Keywords: Magnotostriction, finite element, Fast Fourier Transformation, smart materials, magnetic response

1. Introduction

In many physical problems, coupled fields namely mechanical, electrical and magnetic effects occur simultaneously. Due to inherent complexity, relatively few solutions to such coupled field problems are available in the literature. When electrical field is not considered then it leads to the phenomenon of magnetostriction. Recently for sensing and control of flexible structures such as beams, shells and plates, a magnetostrictive material is being used as it is sensitive to the dynamic characteristics of the structures on which it is mounted.

In general, the phenomenon of magnetostriction is defined as the relation between mechanical and magnetic fields in a body. This phenomenon was discovered by Joule in 1842 [1]. Some magnetostrictive ceramics can be listed as $CoFe_2O_4$, Ni, Alfenol and TerfenolD. Thin films with high magnetostriction are very attractive for active mechanical actuators. The modeling of magnetostrictive thin films and application to a micro membrane was presented by Body et al. [1]. Various piezoelectric/magnetostrictive composite combinationswere formed by Avellaneda and Harshe [2] to calculate the magnetoelectric coefficient and parameters which characterize the efficiency of energy conversion among the layers.

A hybrid device composed of a magnetostrictive film on a piezoelectric substrate was described by Arai et al. [3]. The changes in the properties of the magnetostrictive film were observed as a result of electrical field applications on the piezoelectric substrate. The research pertaining to magnetostriction has increased to a considerable extent over the last decade due to its excellent capabilities of system

*Corresponding author. E-mail: saljahda@gmu.edu.

sensing and control. The variational formulation in terms of magnetic vector potential and displacement is solved for 2D and 3D cases by Besbes et al. [4].

A numerical simulation scheme for magnetostrictive transducers based on magnetic vector potential formulation was proposed by Kaltenbacher et al. [5]. They observed that the coupling of magnetic and mechanical systems induce mechanical strains and permeability changes. Experimental result comparison with the simulations performed for rod actuator gave reasonably accurate results. The deformation of the magnetic material caused by magnetostriction was represented by an equivalent set of mechanical forces by Delaere et al. [6]. The resulting magnetostriction force was superimposed on other force distributions and is the key to the coupling of the magnetic and the mechanical finite element systems. 2D tensor finite element model was used to evaluate force components in magnetostrictive phenomenon by Mohammed [7]. The strains developed due to the presence of magnetic field generates electrical or mechanical forces that are undesirable at low frequencies creating acoustic noise in electromagnetic systems.

Implementation results on a 2hp, permanent motor indicates that magnetostrictive forces are significant and amount to more than 50% force level increase above electromechanical force levels without consideration of magnetostriction. A combined passive and active damping strategy was proposed by Bhattacharya et al. [8]. The performance of giant magnetostrictive materials namely TerfenolD was affected by preloading applied to the material. Finite element simulations on a cantilever beam model were carried out to study dynamic characteristics in combined damping scenario. A novel approach to monitoring and controlling the preloading in a compact giant magnetostrictive positioner was presented by Yamamoto et al. [9]. The proposed method not only provides a means to make a precise measurement of the preloading but also constitutes a sensing capability with which the displacement of the positioner itself can be measured. Finite element analysis was performed to incorporate new design changes to make sure that the giant magnetostrictive element can be driven in an efficient manner.

Sunar et al. [10] demonstrated that a thermopiezomagnetic medium can be formed by bonding together a piezoelectric and magnetostrictive composite. Finite element equations for thermopiezomagnetic media were obtained using linear constitutive equations in Hamilton's principle together with the finite element approximations. It was also shown that an electrostatic field applied to piezoceramic layer causes strain in structure that in turn produces magnetic field in the magnetoceramic layer.

In this paper the constitutive equations are formulated for magnetostriction medium composed of $CoFe_2O_4$ and are mounted on cantilever beam. Finite element method is used to simulate the dynamic response for the composite smart structure subjected to sinosoidal and step force inputs. Application of force generates magnetic field in the magnetostrictive material resulting in magnetic response in X and Y directions. FFT is performed to obtain the PSD response and is used to compare with the displacement response.

2. Constitutive equations of magnetostriction

The following constitutive equations are obtained for a magenetostrictive medium

$$\mathbf{T} = \frac{\partial G}{\partial S} = c\mathbf{S} - l\mathbf{B}$$
$$H = \frac{\partial G}{\partial B} = -l^T\mathbf{S} + \mu^{-1}\mathbf{B} \tag{1}$$

Where c, l and μ^{-1} are the constitutive coefficients, and $\mathbf{T}, \mathbf{S}, \mathbf{H}$ and $\mathbf{B}$ are the vectors of stress, strain, magnetic field intensity and magnetic flux density respectively. The thermodynamic potential $\mathbf{G}$ is given by the following equation

$$G = \frac{1}{2}\mathbf{S}^T c\mathbf{S} + \frac{1}{2}\mathbf{B}^T \mu^{-1}\mathbf{B} - \mathbf{S}^T l\mathbf{B} \tag{2}$$

The generalized Hamilton's principle has the following forms

$$\delta \int_{t_1}^{t_2} (Ki - \Pi)dt = 0 \tag{3}$$

Where Ki is the kinetic energy and π is an energy functional and are given by

$$Ki = \int_V \frac{1}{2}\rho \dot{\mathbf{u}}^T \dot{\mathbf{u}} dt \tag{4}$$

$$\Pi = \int_V GDV - \int_V \mathbf{u}^T \mathbf{P}_{\mathrm{b}} dV - \int_S \mathbf{u}^T \mathbf{P}_{\mathrm{s}} dV + \int_S \mathbf{A}^T H'_E \mathbf{n} dS - \int_V A^T \mathbf{J} dV \tag{5}$$

where $\mathbf{P}_{\mathrm{b}}$ and $\mathbf{P}_{\mathrm{s}}$ are the vectors of body and surface forces; $\mathbf{u}$ and $\mathbf{A}$ are the vectors of mechanical displacement and magnetic potential; $\mathbf{n}$ is the vector normal to the surface, $\mathbf{J}$ is the current density and $\mathbf{H}_{\mathrm{E}}$ is the matrix of external magnetic field intensity and is given by

$$H'_E = \begin{bmatrix} 0 & H_z & -H_y \\ -H_z & 0 & H_x \\ H_y & -H_x & 0 \end{bmatrix}_E \tag{6}$$

The variations in G and Ki are given by

$$\delta G = \delta S^T \mathbf{T} + \delta B^T \mathbf{H} \tag{7}$$

and

$$\delta \int_{t_1}^{t_2} Kidt = -\int_{t_1}^{t_2} dt \int_V \rho \delta \mathbf{u}^T \ddot{\mathbf{u}} dt \tag{8}$$

Substitution of the above equations in Eq. (3) results in the following equation

$$\delta \int_{t_1}^{t_2} (Ki - \Pi)dt = \int_{t_1}^{t_2} dt \left[\int_V (-\rho \delta \mathbf{u}^T \ddot{\mathbf{u}} - \delta \mathbf{S}^T \mathbf{T} - \delta \mathbf{B}^T \mathbf{H} + \delta \mathbf{u}^T \mathbf{P}_b) dV + \int_S \delta \mathbf{u}^T \mathbf{P}_{\mathrm{s}} dS \right.$$
$$\left. - \int_S \delta \mathbf{A}^T H'_E \mathbf{n} dS + \delta \mathbf{A}^T \mathbf{J} \right] dV = 0 \tag{9}$$

Introducing the following relations

$$\mathbf{S} = \boldsymbol{L}_u \mathbf{u} \text{ and } \mathbf{B} = \nabla \times \mathbf{A} = \boldsymbol{L}_A \mathbf{A} \tag{10}$$

Where L_u and L_A are differential operators, and substituting in Eq. (10) in Eq. (9) gives the following equation

$$\int_{t_1}^{t_2} dt \left[\int_V \delta \mathbf{u}^T (-\rho \ddot{\mathbf{u}} + L_{\mathrm{u}}^T \mathbf{T} + \mathbf{P}_{\mathrm{b}}) dV + \int_V \delta \mathbf{A}^T (\mathbf{J} - \nabla \times \mathbf{H}) dV + \right.$$
$$\left. \int_S \delta \mathbf{u}^T (\mathbf{P}_{\mathrm{s}} - N\mathbf{T}) dS - \int_S \delta \mathbf{A}^T (H'_E - H') \mathbf{n} dS) \right] = 0 \tag{11}$$

Finally the following equations are obtained for the mechanical and magnetic fields.

$$-\rho \ddot{\mathbf{u}} + L_{\mathrm{u}}^T \mathbf{T} + P_b = 0, \quad -\nabla \times \mathbf{H} = \mathbf{J} \tag{12}$$

3. Finite element equations for magnetostriction medium

The variables of the finite element formulation are chosen as $\mathbf{u}$ and $\mathbf{A}$ for the mechanical and magnetic fields, respectively. The following approximations are written for each finite element

$$\mathbf{u}_e = N_{\mathrm{u}} \mathbf{u}_i, \quad \mathbf{A}_e = N_A \mathbf{A}_i \tag{13}$$

Where the subscript e and i respectively stand for the element and nodes of the element, and N's are the shape function matrices whose subscripts denote the associated mechanical and magnetic fields. The following relations are also written

$$\mathbf{S}_e = L_{\mathrm{u}} \mathbf{u}_e = [L_{\mathrm{u}} N_{\mathrm{u}}] \mathbf{u}_i = \mathbf{B}_u \mathbf{u}_i$$
$$\mathbf{B}_e = L_A \mathbf{A}_e = [L_A N_A] \mathbf{A}_i = B_A \mathbf{A}_i \tag{14}$$

Finally the following coupled finite element equations are obtained (after assemblage)

$$M_{\mathrm{uu}} \ddot{\mathbf{u}} + C_{\mathrm{u}A} \dot{\mathbf{A}} + K_{\mathrm{uu}} \mathbf{u} - K_{\mathrm{u}A} \mathbf{A} = F$$
$$M_{AA} \ddot{\mathbf{u}} - C_{A\mathrm{u}} \dot{\mathbf{u}} + C_{AA} \dot{\mathbf{A}} - K_{A\mathrm{u}} \mathbf{u} + K_{AA} \mathbf{A} = M \tag{15}$$

Where F and M represent the mechanical force and magnetic current, respectively, $\mathbf{u}$ and $\mathbf{A}$ are the global vectors of displacement and magnetic vector potentials. The element matrices are given by

$$[M_{\mathrm{uu}}]_e = \int_{V_e} N_{\mathrm{u}}^T N_{\mathrm{u}} dV, \quad [K_{\mathrm{uu}}]_e = \int_{V_e} B_{\mathrm{u}}^T c_e B_{\mathrm{u}} dV$$
$$[K_{\mathrm{u}A}]_e = \int_{V_e} B_{\mathrm{u}}^T l_e B_A dV, \quad [K_{AA}]_e = \int_{V_e} B_A^T \mu_e^{-1} B_A dV$$
$$[M_{AA}]_e = \int_{V_e} N_A^T e_e N_A dV, \quad [C_{\mathrm{u}A}]_e = \int_{V_e} B_{\mathrm{u}}^T e_e N_A dV \tag{16}$$
$$[C_{AA}]_e = \int_{V_e} (B_A^T b_e N_A - N_A^T b_e B_A) dV$$

In Eq. (15), $[K_{A\mathrm{u}}] = [K_{\mathrm{u}A}]^T$ and $[C_{A\mathrm{u}} = [C_{\mathrm{u}A}]^T$.

Table 1
Material properties and dimensions of steel beam and magnetostrictive ceramic

Property	Beam	Magnetostrictive Ceramic
Y (Pa)	2.07×10^{11}	1.54×10^{11}
μ_{11}, μ_{33} (H/m)		$6\Pi \times 10^{-8}$
l_{31} (A/m)		2.86×10^{-8}
L (m)	0.125	0.005
t (m)	0.0023	0.0025
w (m)	0.0254	0.0254

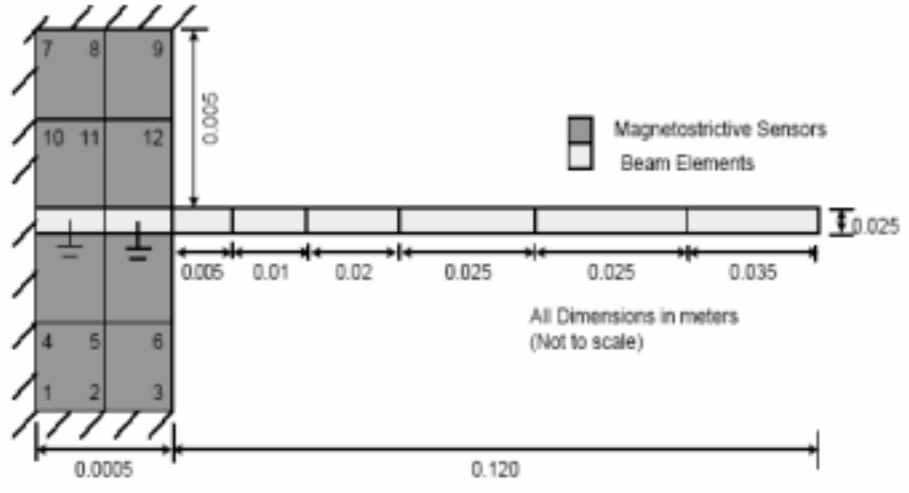

Fig. 1. Finite element model of the composite beam.

4. Case study

A composite beam shown in Fig. 1 is taken as an example to illustrate the use of magnetostriction equations given in previous sections. The cantilever beam is composed of two bonded layers of magnetostrictive layers (CoFe2O4) on the top and bottom at the root of the beam. Material properties of these materials are assumed as in Table 1 [2]. The dimensions of the beam are also given in Table 1.

The beam and the magnetostrictive ceramic are divided into 8 elements. The beam has 2 elements inside the root and 6 outside, and there are 4 magnetostrictive elements meshed above and bottom of the steel beam. There are 26 mechanical degrees of freedom (DOF) and 24 magnetic DOF. A finite element program is written in Matlab to determine the displacement and magnetic response when subjected to different force inputs. For transient response, a step force is applied at the tip of the beam in the vertical upward direction. The vertical tip deflection of the beam and magnetic response generated by the upper sensor at node 9 are computed using Matlab program. The FFT's for these responses are also found through Matlab program. The steady state response of the system is found by applying sinusoidal force at the tip of the beam in the vertical upward direction. The force is assumed to be of the form

$$F = |F| \sin(wt) \tag{17}$$

Where w is the forcing frequency in rad/s. In the present case study w is taken as 20 Hz. The magnetic response is again computed at node 9.

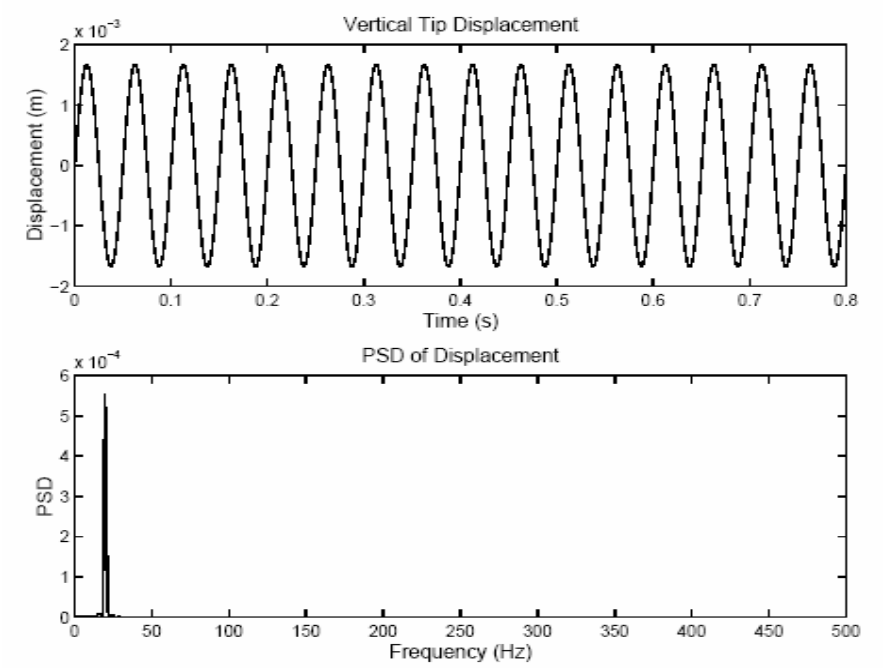

(a)

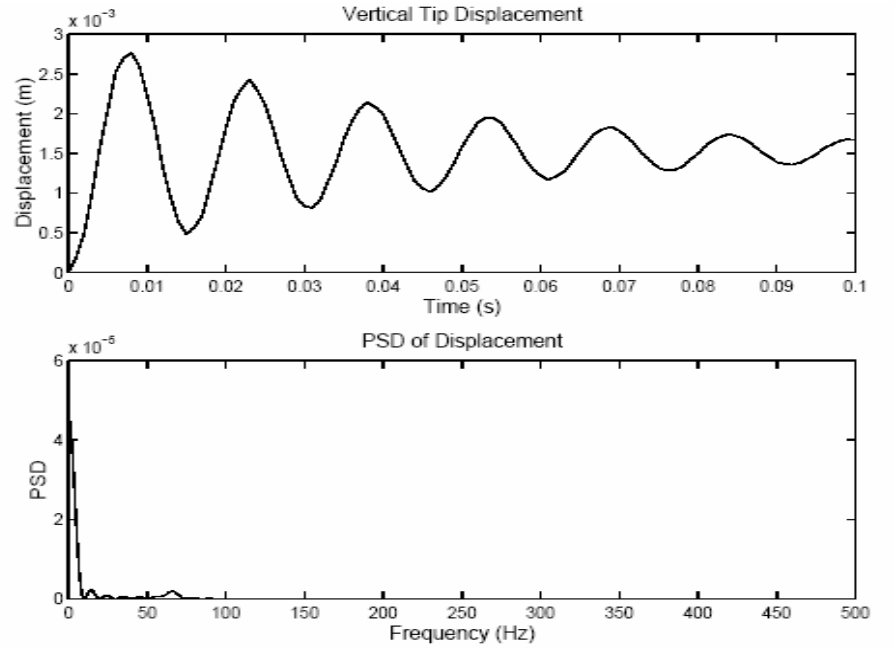

(b)

Fig. 2. (a) Tip displacement and its PSD for sinusoidal force input. (b) Tip displacement and its PSD for step force input.

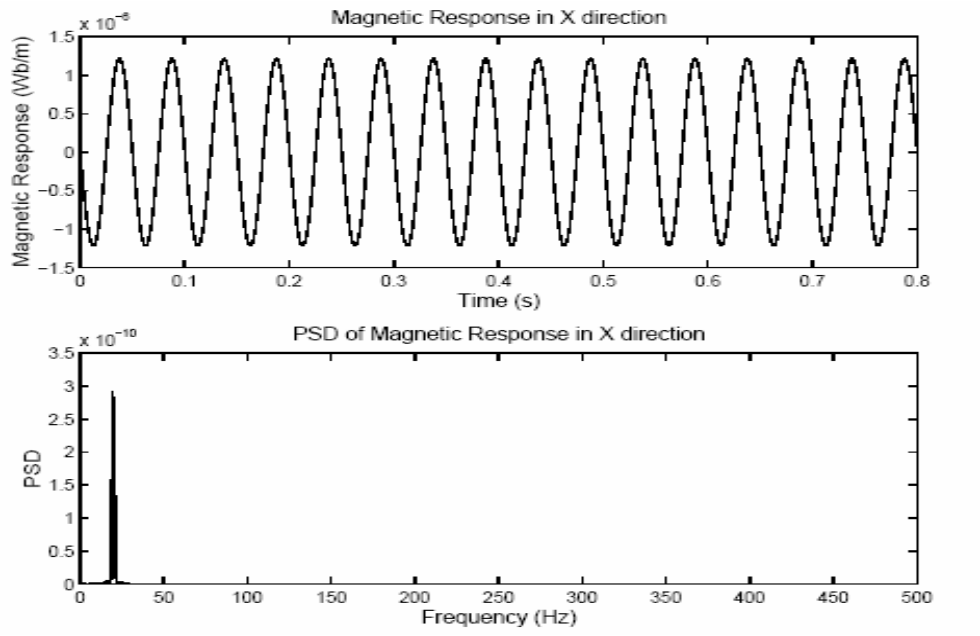

(a)

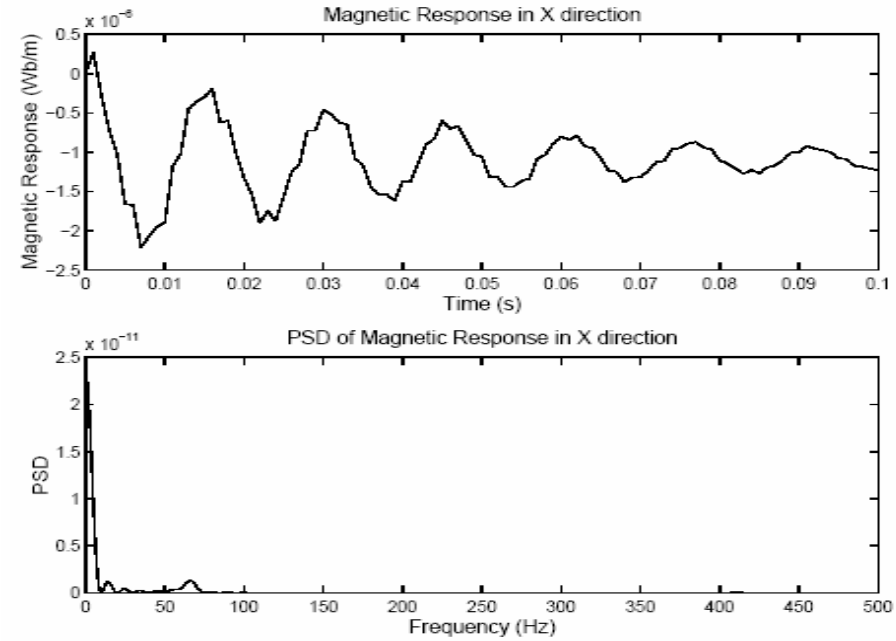

(b)

Fig. 3. (a) Magnetic response and its PSD in X direction for sinusoidal force input. (b) Magnetic response and its PSD in X direction for step force input.

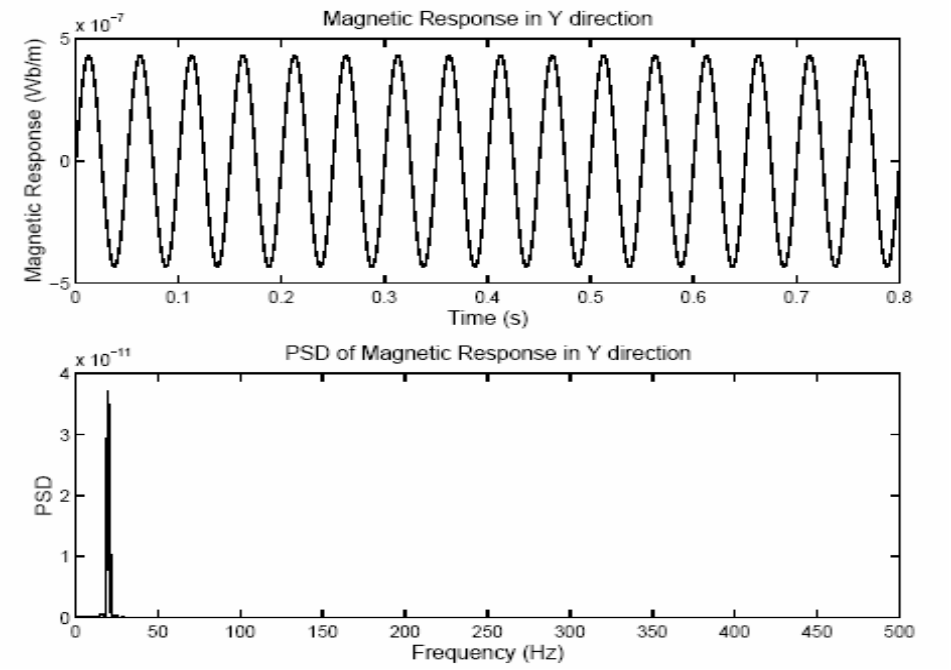

(a)

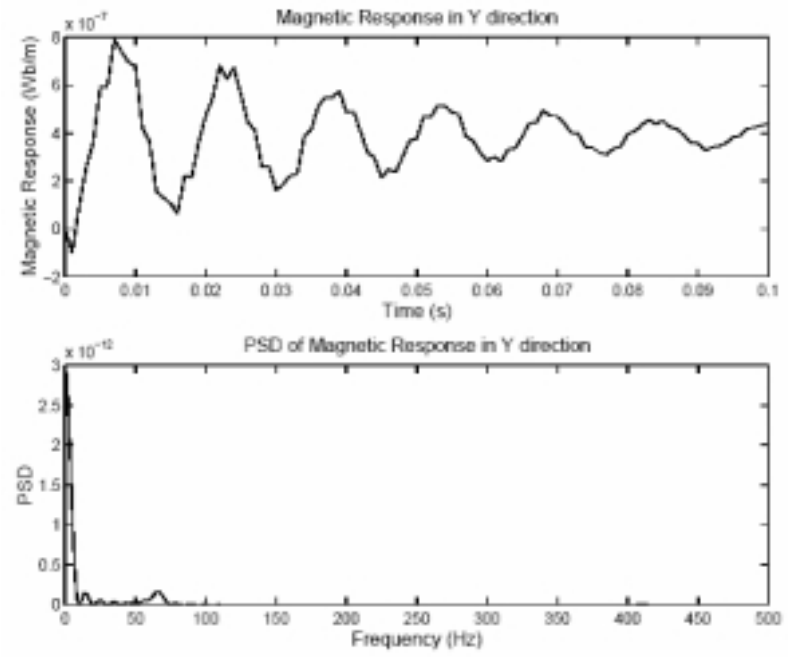

(b)

Fig. 4. (a) Magnetic response and its PSD in Y direction for sinusoidal force input. (b) Magnetic response and its PSD in Y direction for step force input.

5. Results and discussions

Displacement Response: Figure 2a shows the displacement response and the PSD for sinusoidal force input. The response is steady and the response of the output adopts the frequency of the input hence the peak is attained as 20 Hz. Figure 2b shows the displacement response and the PSD for step force input.

The displacement response attains a peak of 2.9 mm and dies down gradually. As expected the PSD is very high initially and the first mode of natural frequency is observed at 60 Hz. The displacement response attains a peak of approximately 3 mm and dies down gradually because of the damping introduced in the system.

Magnetic Response in X direction at node 9: Figure 3a shows the magnetic response in X direction when subjected to sinusoidal force input. The response is steady with a magnitude of 1.25×10^{-5} (Wb/m) and the maximum peak is observed as before at 20 Hz indicating the system is responding with the same frequency as the input frequency. The magnitude of the energy as found from the PSD is 2.75×10^{-8}. Figure 3b shows the magnetic response in X direction for step force input. In contrast to displacement response the magnetic response is negative reaching a peak of -2.25×10^{-5} (Wb/m) at 0.009 s. The PSD response is similar to that of displacement with the peak observed at 60 Hz which is the first natural frequency.

Magnetic Response in Y direction at node 9: Figure 4a shows the magnetic response in Y direction when subjected to sinusoidal force input. The steady response reaches a peak of about 3×10^{-6} (Wb/m) at 20 Hz frequency. The magnitude of energy as revealed by the PSD is $1{:}5 \times 10^{-9}$. Figure 4b shows the magnetic response in Y direction for step force input. The maximum magnetic response is observed at 0.008 s and is of the order of -5.2×10^{-6} (Wb/m). Similar to the discussed two types the maximum peak of PSD is observed at 60 Hz. In general the magnitude of magnetic response in Y direction and its PSD has lesser magnitude than the magnetic response in X direction for all force inputs.

6. Conclusions

The linear constitutive equations of magnetostriction are presented. The differential equations governing the dynamic behavior of a magnetostrictive material are also given. The finite element method is applied to the material to obtain the coupled finite element equations, which are used in modeling and analyzing the numerical example used in the case study.

A cantilever beam together with the pair of a magnetostrictive layer is used in the case study. The displacement as well as magnetic responses obtained as the case study show that a magnetostrictive layer can be used to monitor the transient (step) and steadystate (sinusoidal) responses of the beam in both X and Y directions.

Nomenclature

A Vector of magnetic potential
b Matrix of electromagnetic coefficients
B Vector of magnetic flux density

c Matrix of elastic stiffness coefficients
G Thermodynamic potential
H Vector of magnetic field intensity
I Area moment of inertia about the neutral axis
J Vector of volume current density
L Length of the structure
L Matrix of piezomagnetic stress coefficients
n Vector of surface normal
P Vector of pyroelectric coefficients
$\mathbf{P}_b$ Vector of body forces
$\mathbf{P}_c$ Vector of concentrated forces
$\mathbf{P}_s$ Vector of surface forces
T Thickness
S Strain vector
T Stress vector
u Displacement vector
w Width of the structure
E Matrix of dielectric coefficients
μ Matrix of permeability coefficients
ρ Mass density
ρ_v Volume charge density

References

[1] C. Body, G. Reyne and G. Meunier, Modeling of magnetostrictive thin films, application to a micromembrane, *Journal of Physics III France* **7** (1997), 67–85.
[2] M. Avellaneda and G. Harshe, Magnetoelectric effect in piezoelectric/magnetostrictive multilayer (2-2) composites, *Journal of Intelligent Material Systems and Structures* **5** (1994), 501–513.
[3] K.I. Arai, C.S. Muranaka and M. Yamaguchi, A new hybrid device using magnetostrictive amorphous films and piezoelectric substrates, *IEEE Transactions on Magnetics* **30** (1994), 916–918.
[4] M. Besbes, Z. Ren and A. Razek, A generalized finite element model of magnetostriction phenomena, *IEEE Transactions on Magnetics* **37** (2001), 3324–3328.
[5] M. Kaltenbacher, S. Schneider and H. Landes, Nonlinear finite element analysis of magnetostrictive transducers, *Smart Structures and Materials 2001 – Modeling, Signal Processing and Control in Smart Structures* **4326** (2001), 160–168.
[6] K. Delaere, W. Heylen, R. Belmans and K. Hameyer, Strong magentomechanical fe coupling using local magnetostriction forces, *EPJ Applied Physics* **13** (2001), 115–119.
[7] O.A. Mohammed, Coupled magnetoelastic finite element formulation of anistropic magnetostatic problems, *IEEE SoutheastCon* (2001), 183–187.
[8] B. Bhattacharya, B.R. Vidyashankar, S. Patsias and G.R. Tomlinson, *Active and passive vibration control of flexible structures using a combination of magnetostrictive and ferro-magnetic alloys*, SPIE – International Society for Optical Engineering, 2000, 204–214.
[9] Y. Yamamoto, H. Eda and J. Shimizu, *Application of giant magnetostrictive materials to positioning actuators*, IEEE/ASME International Conference on Advanced Intelligent Mechatronics, 1999, 215–220.
[10] M. Sunar, A.Z. Al-Garni, M.H. Ali and R. Kahraman, *Finite element modeling of thermopiezomagnetic smart structures*, In-Press, September 2002.